Applied Surface Science 347 (2015) 231–241

Contents lists available at ScienceDirect

Applied Surface Science

journal homepage: www.elsevier.com/locate/apsusc

Fluorosilicone multi-block copolymers tethering quaternary ammonium salt groups for antimicrobial purpose

Fang Zhou, Xiaoshuai Qin, Yancai Li, Lixia Ren, Yunhui Zhao*, Xiaoyan Yuan

School of Materials Science and Engineering, and Tianjin Key Laboratory of Composite and Functional Materials, Tianjin University, Tianjin 300072, China

ARTICLE INFO

Article history:
Received 4 February 2015
Received in revised form 10 April 2015
Accepted 10 April 2015
Available online 18 April 2015

Keywords:
Fluorosilicone copolymer
Multi-block
RAFT polymerization
Quaternary ammonium salt
Antimicrobial activity

ABSTRACT

Symmetrically structured fluorosilicone multi-block copolymers containing poly(2-(dimethylamino) ethyl methacrylate) (PDMAEMA) and poly(hexafluorobutyl methacrylate) (PHFBMA) were sequentially synthesized via reversible addition–fragmentation chain transfer polymerization, using a polydimethylsiloxane (PDMS) chain transfer agent with dithiocarbonate groups at both ends. Then, the CBABC-type block copolymers were quaternized with *n*-octyliodide to tether quaternary ammonium salt (QAS) groups in the PDMAEMA blocks for the antimicrobial use. The obtained fluorosilicone copolymers showed clear variations in the C-N^+ composition and surface morphology on their films depending on the content of the PHFBMA blocks, which were characterized by X-ray photoelectron spectroscopy and atomic force microscopy, respectively. The results indicated that the symmetrical CBABC structure favored PDMS and QAS tethered blocks migrating to the film surface. With the mass percentage of the PHFBMA increased from 0 to 32.5%, the surface roughness of the copolymer film decreased gradually with a tendency to form a smooth surface. Owing to the surface properties, fluorosilicone multi-block copolymers containing a certain amount of PHFBMA with higher C-N^+ content and relatively smooth morphology demonstrated obvious antimicrobial activity against Gram-positive bacteria, *Bacillus subtilis* and Gram-negative bacteria, *Escherichia coli*. The functionalized multi-block copolymers based on fluorosilicone and QAS groups would have potential applications in antimicrobial coatings.

1. Introduction

Increasing concerns of infections and diseases emphasize the importance of preventing the growth of microorganisms and great efforts have been made to develop materials with significant antimicrobial activity [1,2]. To inhibit the microbial colonization on a surface, one of the most active methods is to kill bacteria with a wide range of antimicrobial materials or drugs, such as silver ions, cationic polymers, antimicrobial peptides and antibiotics [3–6]. Among them, polymers containing quaternary ammonium salt (QAS) groups are the most widely used cationic materials to inhibit microbial growth and are effective at killing a broad spectrum of microorganisms [7–10]. It is well known that poly(2-dimethylaminoethyl methacrylate) (PDMAEMA) with tertiary amino groups can be further converted into a cationic polymer with QAS groups, which has been considered to be a promising polymeric antimicrobial agent [7]. It is considered that the antimicrobial activity provided by QAS comes from both cationic and hydrophobic interactions occurring between the quaternized groups and the counterpart of the microbial cell walls. For this proposed mechanism, there would be a loss of the integrity in the bacterial cytoplasmic membranes as well as other damaging effects to the bacterial cells [9,10].

Fluorinated polymers exhibits excellent properties, such as low surface energy, low friction coefficient, good biocompatibility, and excellent thermal as well as chemical resistances. Undoubtedly, fluoropolymers can be used as antifouling coatings and surface modification for the antimicrobial purpose [6,11,12]. Thorpe et al. reported the synthesis of poly(methylpropenoxyfuoroalkylsiloxane)s, a class of fluorosilicone materials, which are inherently resistant to bacterial colonization [11]. Cai et al. reported the fabrication of biofunctionalized fluoropolymers via fluorous interactions and “click” chemistry to immobilize an antimicrobial peptide on the fluorous thin films and fluorosilicone contact lens [6]. Particularly, fluorosilicone block copolymers containing polydimethylsiloxane (PDMS) and fluorocarbon segments which combine advantages of both siloxane and fluorinated polymers, are excellent in performances like low surface energy, chemical resistance and weather resistance

* Corresponding author. School of Materials Science and Engineering, Tianjin University, Tianjin 300072, China, Tel./fax: +86 22 8740 1870.
E-mail address: zhaoyunhui@tju.edu.cn (Y. Zhao).

http://dx.doi.org/10.1016/j.apsusc.2015.04.079
0169-4332/

[13,14]. Martinelli et al. prepared amphiphilic copolymers involving PDMS and polyacrylate units with mixed PEGylated-fluoroalkyl side chains. They demonstrated that the fluoroalkyl segments of the copolymer migrated towards the film surface, dragging the linked PEGylated groups to the surface, which brought about surface structure for fouling release application [15].

Block copolymers have been studied intensively, concerning the possible self-assembly in both bulk and selective solution [7,16–20]. The self-assembled structures therefore have potential applications in antimicrobial materials [7,18], antifouling surfaces [13,20] and gene delivery systems [16]. Among the approaches for structuring copolymers, reversible addition-fragmentation chain transfer (RAFT) polymerization is often adopted to produce block copolymers with controlled molecular mass, narrow polydispersity and well-defined structure for antimicrobial purpose [7,19]. The well-defined copolymers can generate special composition and unique morphology on film surfaces, which allows greater insight into the structure-antimicrobial activity relationship.

In our previous research, a series of PDMS-*b*-QPDMAEMA (quaternized PDMAEMA) block copolymers were synthesized via RAFT polymerization and quaternization, which indicated that the antimicrobial activity was highly dependent on the surface with heterogeneous morphology and higher N^+ content [21]. Following the aforementioned studies, fluorosilicone methacrylate multi-block copolymers containing fluoroalkyl and QAS groups were conceived to tailor surface structures. For the purpose of finding an economic and practical biomedical antimicrobial coating in this study, a series of CBABC-type multi-block copolymers containing PDMS, PDMAEMA and poly(hexafluorobutyl methacrylate) (PHFBMA) were synthesized via RAFT polymerization and quaternization, taking the effects of charge density and surface morphology on antimicrobial efficiency into account. PDMS was used as macro chain transfer agent (CTA-PDMS-CTA) with dithiocarbonate groups at both of its terminals. PHFBMA was used as a modified composition with low surface energy and film-forming ability, while QPDMAEMA was designated to fulfill the antimicrobial function. It was hypothesized that tailoring PHFBMA block with controlled chain length via RAFT polymerization would provide a unique method for investigating the effects of fluorinated blocks on the surface composition variation and surface morphology of copolymer films. With regard to structure–antimicrobial relationships, the antimicrobial activity of the copolymer films was determined using Gram-positive bacteria, *Bacillus subtilis* (*B. subtilis*) and Gram-negative bacteria, *Escherichia coli* (*E. coli*), respectively.

2. Experimental methods

2.1. Materials

α,ω-Dihydride-terminated PDMS (H-PDMS-H, M_n = 2000) was supplied by Hangzhou Silong Material Technology Co., Ltd., China. 2,2,3,4,4,4-Hexafluorobutyl methacrylate (HFBMA) was supplied by Xeogia Fluorin-Silicon Chemical Co., Ltd., China. 2-(Dimethylamino)ethyl methacrylate (DMAEMA, 98%) and *n*-octyliodide were obtained from Sigma-Aldrich. 2,2′-Azobisisobutyronitrile (AIBN, Shanghai Chemical Reagent, 98%) was recrystallized in ethanol and kept in a refrigerator at 4 °C. Hydroxyethyl methacrylate (HEMA) and solvents including methanol, acetonitrile, ethyl acetate and hexane were obtained from Tianjin Kemiou Chemical Reagent Co., Ltd., China. α,α,α-Trifluorotoluene (TFT) was purchased from Tianjin Heowns Biochem Technologies LLC, Tianjin, China. Hexamethylene diisocyanate (HDI) was supplied by Bayer AG, Germany. The monomers (DMAEMA, HFBMA, and HEMA) were purified by passing though a neutral alumina column prior to use and other reagents were used as received. Gram-positive bacteria (*B. subtilis*, ATCC 63501) and Gram-negative bacteria (*E. coli*, ATCC 44752) were supplied by Hebei University of Science and Technology, China, and were incubated at 4 °C on nutrient agar plates.

2.2. Synthesis of PDMS-b-(PDMAEMA)$_2$

4-Cyanopentanoic acid dithiobenzoate (CPADB) and α,ω-(hydroxy propyl) PDMS (M_n = 2204 from the gel permeation chromatography measurement) were firstly prepared according to the references, respectively [22,23]. And then, PDMS macro chain transfer agent (CTA-PDMS-CTA) was synthesized according to the literature [24] as shown in Scheme 1.

The synthesis procedure for PDMS-*b*-(PDMAEMA)$_2$ is also described in Scheme 1. RAFT polymerization was conducted in a 50 mL dry three necked flask equipped with a magnetic stirrer. The initial molar ratio of [DMAEMA]:[CTA-PDMS-CTA]:[AIBN] was set as 130:1:0.2. In a typical reaction, DMAEMA (2.041 g, 13 mmol), CTA-PDMS-CTA (0.273 g, 0.1 mmol) and AIBN (3.28 mg, 0.02 mmol) were dissolved in toluene (2.3 g) and deoxygenated by bubbling with nitrogen. Then, the reaction was carried out under stirring in a water bath at 65 °C for 12 h and stopped by quenching to 0 °C. The crude product was diluted and dialyzed against methanol over 48 h. After dialysis, methanol was removed by rotary evaporator and the obtained copolymer was dried under high vacuum at room temperature for 24 h to give rise to the BAB triblock copolymer PDMS-*b*-(PDMAEMA)$_2$ (simplified as PDMS-PM).

2.3. Synthesis of PDMS-b-[PDMAEMA-b-PHFBMA-b-P(HFBMA-co-HEMA)]$_2$

The prepared copolymer PDMS-PM was further used as the macro chain transfer agent to mediate the sequential polymerization of HFBMA and HEMA. Typically, the initial molar ratio of [HFBMA]:[HEMA]:[PDMS-PM]:[AIBN] was set as 100:20:1:0.2. HFBMA (1.0 g, 4.0 mmol), PDMS-PM (0.6 g, 0.04 mmol) (M_n = 15.3 kDa) and AIBN (1.31 mg, 0.008 mmol) were dissolved in TFT (1.6 g) in a 50 mL three neck flask. The solution was then degassed to remove oxygen, and polymerization was conducted in water bath at 65 °C for 10 h. A certain amount of HEMA was additionally added for crosslinking. The reaction was stopped by quenching to 0 °C and exposure to air. The mixture was diluted and dialyzed against methanol. After dialysis, methanol was removed by rotary evaporator, and the product was dried under vacuum at room temperature for 24 h to obtain the multi-block copolymers PDMS-*b*-[PDMAEMA-*b*-PHFBMA-*b*-P(HFBMA-*co*-HEMA)]$_2$ (abbreviated as PDMS-PM-PF). The BAB triblock copolymer PDMS-PM$_{80}$ and the CBABC multi-block copolymers with three different contents of the PHFBMA blocks, i.e. PDMS-PM$_{80}$-PF$_{30}$, PDMS-PM$_{80}$-PF$_{52}$ and PDMS-PM$_{80}$-PF$_{70}$, were synthesized as shown in Table 1.

2.4. Quaternization of multi-block copolymer

The quaternization of the multi-block copolymers were carried out in a 50 mL dry three-necked flask equipped with a magnetic stirrer. In a typical reaction, PDMS-PM-PF copolymer (1.0 g, 3.25 mmol tertiary groups) and *n*-octyliodide (1.1 g, 4.55 mmol iodide ions) were dissolved in acetonitrile, and the quaternization reaction was performed at 70 °C for 32 h. The crude product was precipitated in hexane three times. The quaternized copolymer PDMS-*b*-[PDMAEMA-*b*-P(DMAEMA-*co*-HEMA)]$_2$ was denoted as PDMS-QPM, and the multi-block copolymer PDMS-*b*-[PDMAEMA-*b*-PHFBMA-*b*-P(HFBMA-*co*-HEMA)]$_2$ was denoted as PDMS-QPM-PF after quaternization. Quaternized PDMS-QPM$_{80}$ and multi-block copolymers with three different mass percentages

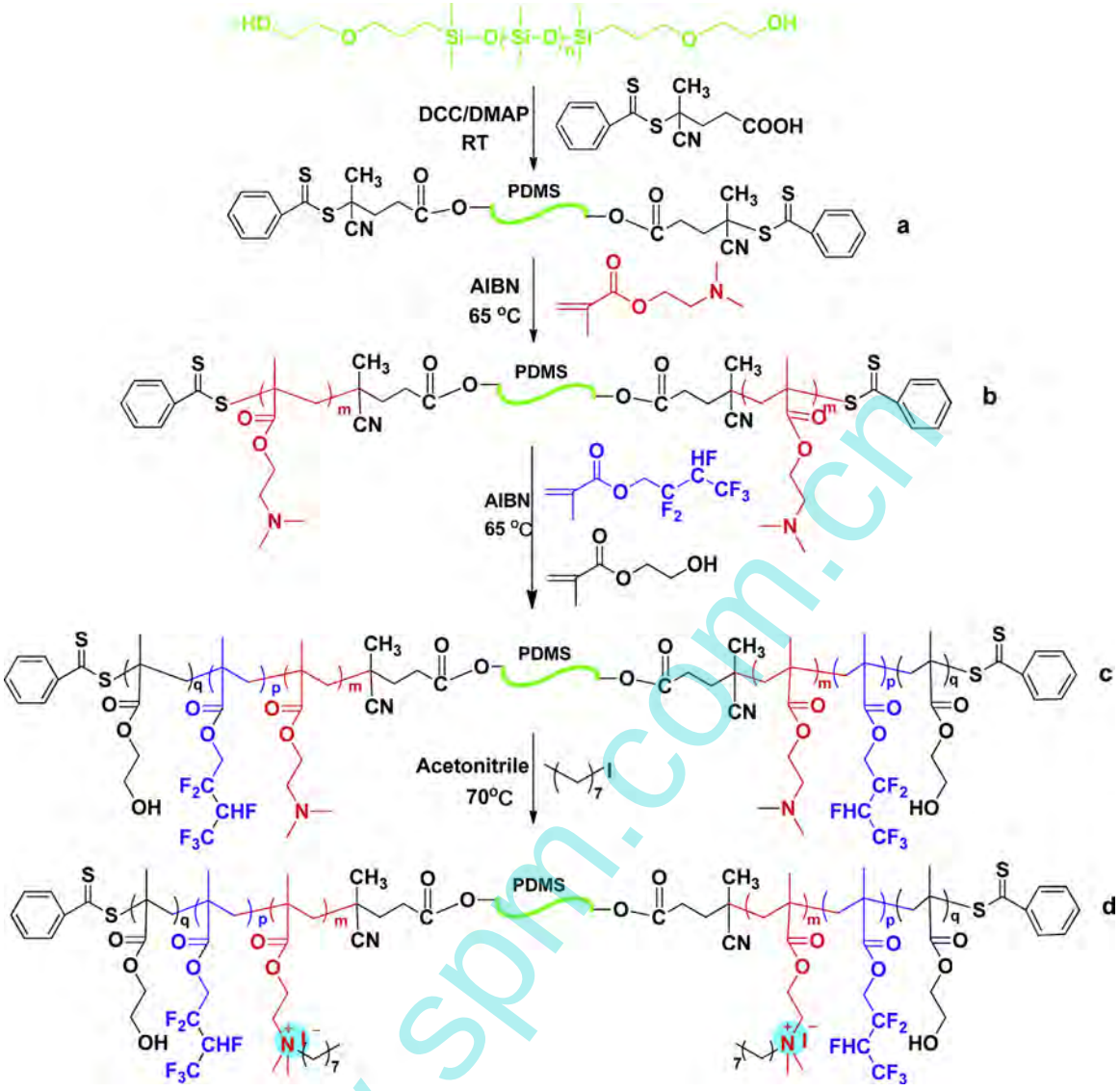

Scheme 1. Synthesis and quaternization of the multi-block copolymers. (a) CTA-PDMS-CTA, (b) PDMS-PM, (c) PDMS-PM-PF and (d) PDMS-QPM-PF.

Table 1
Conversion and molecular mass of the prepared multi-block copolymers.

Sample	^{1}H NMR				GPC		f_{PHFBMA} [b] (wt%)
	Conv.$_{DMAEMA}$ (%)	*Conv.*$_{HFBMA}$ (%)	Reaction time of HFBMA (h)	M_n [a] (kDa)	M_n (kDa)	PDI	
PDMS-PM$_{80}$	61.5	0	0	15.3	15.1	1.15	0
PDMS-PM$_{80}$-PF$_{30}$	–	30.2	5.0	24.6	23.9	1.21	17.1
PDMS-PM$_{80}$-PF$_{52}$		52.2	8.5	30.6	28.5	1.25	26.1
PDMS-PM$_{80}$-PF$_{70}$		70.4	12.0	34.6	32.4	1.26	32.5

[a] Calculated from the conversion as follows: $M_{n,NMR}$ = [HFBMA]/[PDMS-PM] × M_{HFBMA} × *Conv.*$_{PHFBMA}$ (%) + $M_{PDMS-PM}$ + M_{HEMA} × 15, where, M_{HFBMA}, $M_{PDMS-PM}$ and M_{HEMA} are referred to the molecular weight of HFBMA, PDMS-PM and HEMA, respectively, and "15" is the repeat unit number of HEMA in PDMS-PM-PF by ^{1}H NMR.
[b] Mass percentage of the PHFBMA block in the quaternized copolymers.

of the PHFBMA blocks (f_{PHFBMA}), i.e. PDMS-QPM$_{80}$-PF$_{30}$, PDMS-QPM$_{80}$-PF$_{52}$ and PDMS-QPM$_{80}$-PF$_{70}$, were prepared. And the f_{PHFBMA} values of different quaternized block copolymers are displayed in Table 1.

2.5. Preparation of multi-block copolymer films

A certain amount of the obtained block copolymers and HDI were dissolved in a mixed solvent of acetonitrile and TFT (v/v = 7/3) to prepare the copolymer solution (10 wt%). Then, the solution (200 μL) was spin-coated on clean aluminum sheets (2 cm × 2 cm) in the conditions of rotating speeds at 600 r/s for 6 s firstly and followed 3000 r/s for 10 s. The solvent was evaporated at room temperature for 1 h before the samples were cured in an oven at 100 °C for 2 h. The thicknesses of the obtained copolymer films were around 0.5 μm. These films were used for the characterization of surface structure and antimicrobial activity testing.

2.6. Characterizations

^{1}H nuclear magnetic resonance (^{1}H NMR) spectra of samples were recorded on a Varian spectrometer (INOVA 500 MHz and

Infinity plus 300WB, USA) in deuterated chloroform ($CDCl_3$) at room temperature.

The average relative molecular mass and its distribution of the prepared block copolymers were determined in gel permeation chromatography (GPC, TDA305, Malvern Instruments Ltd., UK) equipped with a Waters 2414 refractive index detector. THF was used as the eluent with a flow rate of 1.0 mL min^{-1} at 40 °C, and monodisperse polystyrene standards were used for calibration.

Differential scanning calorimetry (DSC) was carried out in a TA instrument (DSC F1 204, Germany) under a nitrogen atmosphere. For measuring the glass transition temperature (T_g), samples were heated from ambient temperature to 120 °C at the heating rate of 40 °C min^{-1}, and then cooled to −150 °C at the cooling rate of 10 °C min^{-1}, followed by reheating from −150 °C to 120 °C at the heating rate of 10 °C min^{-1}. The thermograms in the second heating run were recorded. An empty aluminium pan was used as reference.

X-ray photoelectron spectroscopy (XPS) was performed on a Perkin-Elmer PHI 5000 C ECSA X-ray photoelectron spectroscopy in ultra-high vacuum with Al K radiation (1486.6 eV) operating at 24.2 W under vacuum. The specimens were analyzed at an electron take off angle of 45° and the tested area was a circle in 100 μm diameter. XPSPEAK41 software was used for the analysis of all the XPS spectra.

Atomic force microscope (AFM) images were investigated using tapping mode on a CSPM5500A of Being Nano-Instruments equipped with E-type vertical engage piezoelectric scanner, China. Cleaned silicon wafers were obtained by rinsing them with ethyl alcohol. The AFM samples were prepared by spin-coating the solution of block copolymers onto the cleaned silicon wafers. Samples were imaged at 3 μm × 3 μm magnifications using a nanosensor silicon tip.

The surface morphology of the crosslinked films was also studied by scanning electron microscopy (SEM, Hitachi S-4800, Japan). The copolymer film samples were coated with a gold layer using Leica EM ACE200 sputter coating unit.

Static water contact angles (CA) on various films were measured at room temperature using JC2000D contact angle goniometer from Shanghai Zhongchen Equipment Ltd., China. Briefly, a water drop (ca. 5 μL) was lowered onto the dry film surface with a microsyringe and then the CA value was recorded after 3 s. In this study, *n*-hexadecane and deionized water were chosen as the nonpolar and polar liquids, respectively, for the measurement of surface energy of the films by using Owens–Wendt–Kaelble method [17]. The measurement of water contact angle hysteresis (CAH) was carried out using 5 μL water droplets which expanded and shrunk by 10 μL at 0.1–1.0 μL/s via a needle from a syringe. Images of the droplets were captured by a CCD camera and analyzed to obtain the advancing and receding contact angles, and values of the water contact angle hysteresis were calculated [9]. The data presented are the average of five measurements on more than three different samples.

2.7. Assessment of antimicrobial activity

The antimicrobial property of the copolymer films was assessed with an agar plating method according to the references [1,8], which was also adopted to evaluate organic silicone resin with QAS groups [9,25]. For these experiments, initial bacteria concentration was set approximately 10^5–10^6 CFU/mL. 200 μL of initial bacteria was added on the nutrient agar plates and ensured the uniform distribution on the surface. A sterile swab was used to inoculate a lawn for each of bacteria on their corresponding agar plates. The coated aluminum discs were then placed on the agar plates with the coated side in direct contact with the agar surface. The plates were inverted and incubated for 24 h at 37 °C. Inhibition of microbial growth around film surfaces was evaluated visually from digital images taken after 24 h of incubation. For different bacteria, a transparent inhibition zone surrounding the coated specimen was designated as "+" for antimicrobial response. Conversely, if films showed no inhibition zone, the antimicrobial response was given the designation "−".

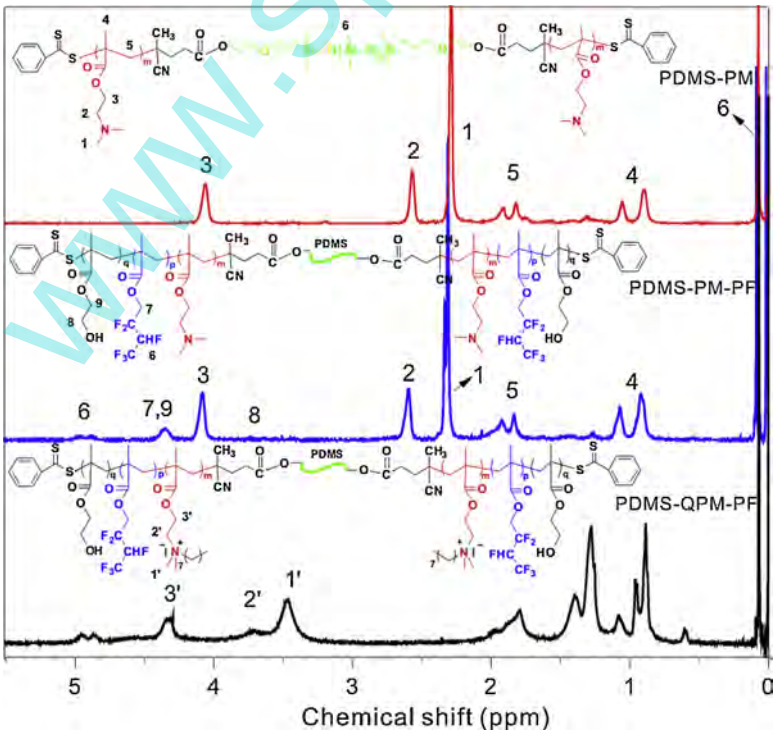

Fig. 1. ^{1}H NMR spectra of the synthetic multi-block copolymers.

3. Results and discussion

3.1. Synthesis of PDMS-PM-PF and PDMS-QPM-PF multi-block copolymers

The multi-block copolymers PDMS-*b*-[PDMAEMA-*b*-PHFBMA-*b*-P(HFBMA-*co*-HEMA)]$_2$, i.e. PDMS-PM-PF were prepared via sequential RAFT polymerization of DMAEMA and HFBMA plus HEMA. And, the block copolymers were quaternized with *n*-octyliodide to prepare PDMS-QPM-PF tethering QAS groups as shown in Scheme 1.

Fig. 1 shows the typical ^{1}H NMR spectra of PDMS-PM, PDMS-PM-PF and PDMS-QPM-PF. Characteristic peaks of the PDMAEMA blocks appear at 2.6 ppm (—OCH$_2$C***H***$_2$N(CH$_3$)$_2$) and 2.3 ppm (—CH$_2$CH$_2$N(C***H***$_3$)$_2$). The signals for PDMS-PM-PF at 5.0 ppm and 4.9 ppm are attributed to the protons of -CHF- groups, and the signal at 4.3 ppm corresponds to the protons of methylene adjacent to the oxygen atom in PHFBMA. Compared with PDMS-PM-PF, PDMS-QPM-PF exhibits specific signals at 3.5 ppm (—N$^+$(C***H***$_3$)$_2$) and 3.7 ppm (—C***H***$_2$N$^+$(CH$_3$)$_2$—) due to the quaternization of the PDMAEMA blocks. Moreover, the signal of methylene protons (—COOC***H***$_2$CH$_2$N$^+$—) was also shifted from 4.1 ppm to 4.4 ppm, which demonstrates that the copolymers tertiary amino groups have almost been transformed into QAS groups [7,26]. The conversion of the first polymerized monomer DMAEMA was measured by comparing the integral intensity in ^{1}H NMR spectra at 2.3 ppm ascribed to —N(C***H***$_3$)$_2$ in PDMAEMA with that at 0.2 ppm belonged to —C***H***$_3$ for CTA-PDMS-CTA agents. In the same way, the conversion of the monomer HFBMA was measured in ^{1}H NMR spectra by comparing the integral intensities at 5.0 ppm and 4.9 ppm due to —C***H***F— of PHFBMA with that at 0.2 ppm for CTA-PDMS-CTA.

For comparison, four multi-block copolymers, namely, PDMS-PM$_{80}$, PDMS-PM$_{80}$-PF$_{30}$, PDMS-PM$_{80}$-PF$_{52}$ and PDMS-PM$_{80}$-PF$_{70}$, with different percentages of fluorinated HFBMA monomers were synthesized. The relative molecular mass, conversion and polydispersity index (PDI) of the prepared multi-block copolymers are summarized in Table 1.

The GPC traces of the fluorosilicone multi-block copolymers were highly symmetrical with narrow polydispersity as shown in Fig. 2. As the polymerization of HFBMA proceeded, the multi-block

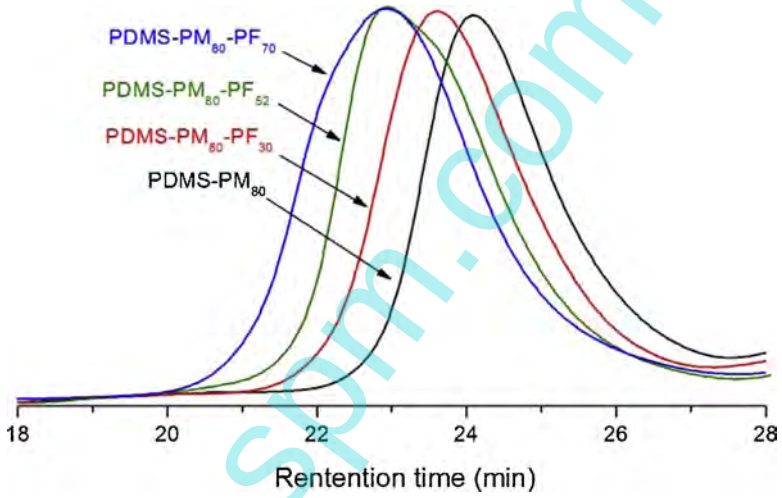

Fig. 2. GPC curves of the multi-block copolymers obtained by RAFT polymerization.

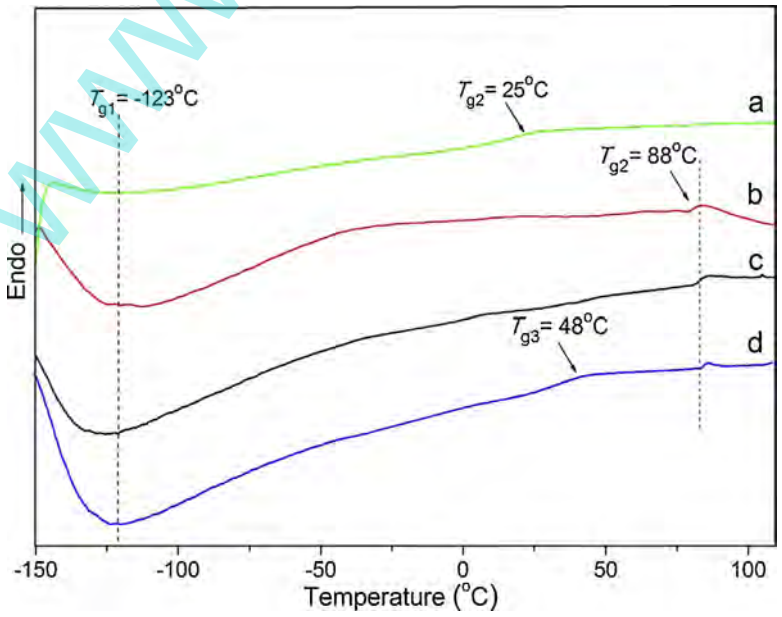

Fig. 3. DSC curves of the multi-block copolymers. (a) PDMS-PM$_{80}$, (b) PDMS-QPM$_{80}$, (c) PDMS-QPM$_{80}$-PF$_{52}$ and (d) PDMS-QPM$_{80}$-PF$_{70}$.

copolymers were prepared in a controlled manner with the molecular mass in range of 15 kDa–35 kDa and PDI less than 1.26. The results revealed that PDMS-PM (PDI = 1.15), the first resultant of the RAFT polymerization, was an effective macro-RAFT agent to mediate further polymerization of HFBMA.

3.2. Thermal behaviors of the multi-block copolymers

Fig. 3 shows the DSC heating curves of the copolymers. As shown in Fig. 3, each copolymer exhibits a glass transition temperature at about −123 °C (T_{g1} = −123 °C), typically observed for PDMS. And, before quaternization, the glass transition temperature T_{g2} at 25 °C associated with the PDMAEMA blocks was detected in PDMS-PM$_{80}$ [Fig. 3(a)]. Meanwhile, after quaternization, samples PDMS-QPM$_{80}$, PDMS-QPM$_{80}$-PF$_{52}$ and PDMS-QPM$_{80}$-PF$_{70}$ displayed the increased glass transition temperatures of T_{g2} around 88 °C for the QPDMAEMA blocks [Fig. 3(b–d)], which could be attributed to the counter ion groups that affected the compliance of the copolymer segments [27]. An additional glass transition temperature T_{g3} at 48 °C associated with the PHFBMA blocks was detected for PDMS-QPM$_{80}$-PF$_{70}$ containing about 32.5 wt% PHFBMA in Fig. 3(d). The copolymer PDMS-QPM$_{80}$-PF$_{52}$ did not show its T_{g3}, due to the less amount of PHFBMA (ca. 26.1 wt%). The occurrence of several glass transition temperatures in each heating run indicated the potential microphase separation among the blocks within the copolymers.

3.3. Chemical compositions of the multi-block copolymer films

In order to obtain robust copolymer films, the multi-block copolymers were crosslinked by HDI. Atomic surface concentrations for PDMS-QPM-PF copolymer films determined by XPS allowed us to describe atomic surface distribution in depth (ca. 10 nm) on the surfaces. The peaks of C 1s (283.7 eV), O 1s (531.2 eV), Si 2s (152.6 eV), Si 2p (101.3 eV), N 1s (399.8 eV) and I 3d5 (624.5 eV) were all detected in each copolymer film. Fluorinated methacrylate polymers, such as PHFBMA were detected the F 1s signals at binding energy around 687 eV and 689.0 eV, respectively [14,15]. Similarly, the binding energy of F 1s was measured at 687.9 eV for PHFBMA in this study and the experimental data were summarized in Table 2. For comparison, the theoretical values calculated from the chemical formula of the copolymer in bulk were reported in Table 2. As shown in Table 2, surface enrichment of the fluorine element was detected from 0 to 4.3% with the increased mass percentage of the PHFBMA blocks, which was not obvious with respect to the normal contribution in bulk from 0 to 13.8%. Alternatively, both silicon and nitrogen element contents on the surfaces were higher than those in bulk for all the multi-block copolymers, i.e. PDMS and the QPM blocks had a stronger tendency on surface segregate than the polyfluoroalkyl blocks did. This phenomenon was related to symmetrical CBABC structure of the present multi-block copolymers. As shown in Scheme 1, the PDMS block locates in the middle of the copolymer chain and its segment can be easily migrated to the surface due to far away from the crosslinking sites (junction zones) and less affected by steric hindrance. In contrast, the PHFBMA blocks were dragged by the junction zones and difficult to migrate to the surface. Another reason was the relatively short fluorinated side chains in the PHFBMA blocks, which showed weaker migration ability to surface [28].

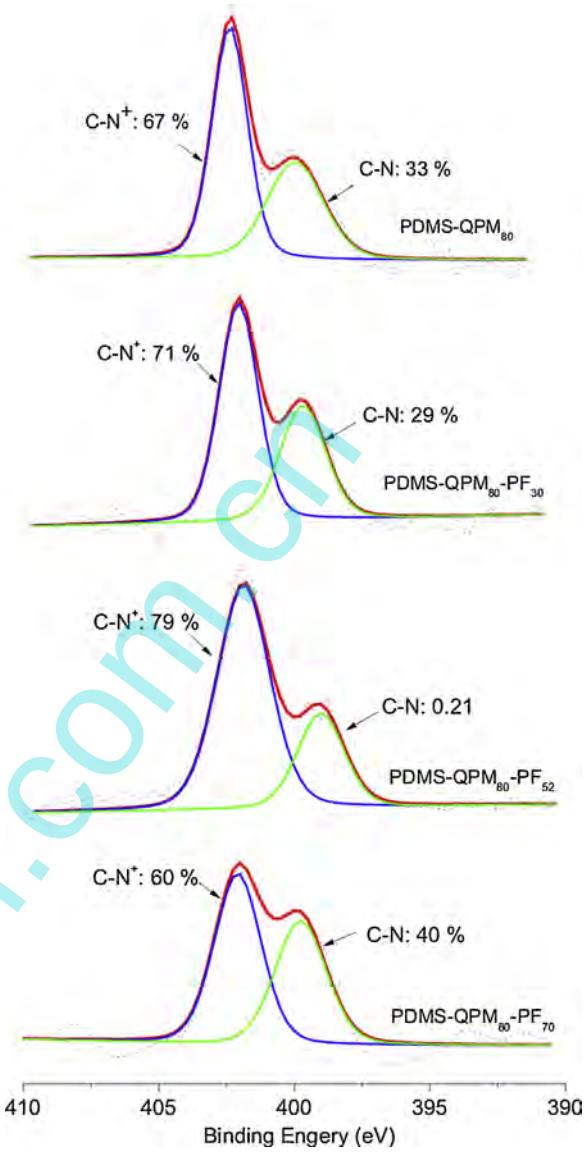

Fig. 4. High resolution N 1s XPS spectra of the multi-block copolymer films.

The high resolution XPS spectra of the N 1s for fluorosilicone copolymer films are shown in Fig. 4. The XPS results indicated that the presence of N 1s peaks were resolved into C-N$^+$ and C—N, which appeared at 402.3 eV and 399.6 eV, respectively, and the percentages of C—N$^+$ and C—N were also shown in Fig. 4. With the mass percentage of PHFBMA increased from 0 to 26.1 wt %, the migration probability of PHFBMA blocks to surface is enhanced,

Table 2
Element composition on the film surfaces by XPS and in bulk of the multi-block copolymers.

Sample	Element composition on the surface by XPS						Element composition in bulk [a]		
	C 1s (%)	O 1s (%)	Si 2p (%)	N 1s (%)	I 3d5 (%)	F 1s (%)	F content (%)	Si content (%)	N content (%)
PDMS-QPM$_{80}$	70.8	15.9	4.6	4.7	4.0	–	–	1.4	4.1
PDMS-QPM$_{80}$-PF$_{30}$	67.9	16.8	5.1	4.1	3.4	2.7	7.5	1.1	3.3
PDMS-QPM$_{80}$-PF$_{52}$	67.9	16.0	5.2	3.5	4.0	3.4	11.3	1.0	2.9
PDMS-QPM$_{80}$-PF$_{70}$	65.7	17.2	5.6	4.5	2.7	4.3	13.8	0.9	2.6

[a] The element composition in bulk was estimated from the chemical structure of the multi-block copolymers.

dragging more adjoining QAS related blocks towards surface. As a result, there was a slight increase in the percentage of C—N^+ on film surfaces accompanying with the fluorine element variation from 0 to 3.4% in Table 2. However, when the percentage of PHFBMA increased to 32.5 wt%, excessive PHFBMA in the copolymer could hinder surface segregate of the QAS tethered segments. Therefore, the surface percentage of C—N^+ corresponded to C—N decreased to 60% for the PDMS-QPM_{80}-PF_{70} sample as shown in Fig. 4.

As shown in Fig. 4, the surface percentages of C—N^+ were all above 60% for the multi-block copolymer films. Considering the quaternization reaction was almost completely according to the ^{1}H NMR results, it was assumed that the C—N content on the surface was mainly generated from the crosslinker HDI. It would be expected that the amine groups on the film surface would be readily quaternized in each case, and it would be the most important for the antibacterial activity [29].

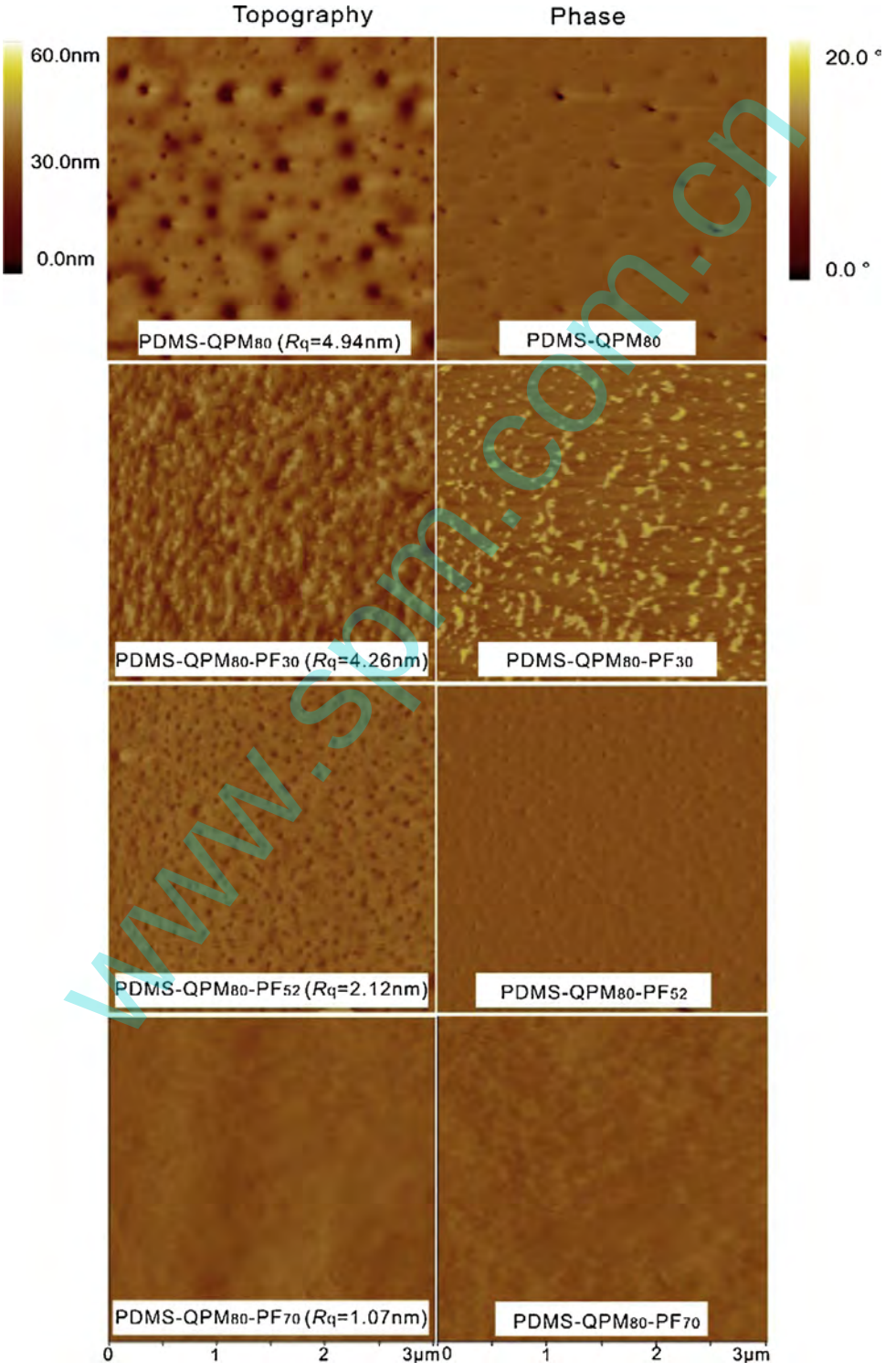

Fig. 5. AFM topography and phase images of the multi-block copolymer films.

3.4. Morphology of the multi-block copolymer films

The migration of the fluorinated moieties to the air-surface of the film can affect the surface roughness [30], and this phenomenon can also be witnessed by AFM. In Fig. 5, all the copolymer films exhibit obvious variations in surface roughness. As mass percentage of PHFBMA increased from 0 to 32.5 wt%, the surface roughness of root mean square (R_q) value decreased gradually from 4.94 nm to 1.07 nm. Additionally, deep valleys were observed in PDMS-QPM$_{80}$ [Fig. 5], while other copolymer films containing PHFBMA presented relatively smoother surfaces. The intermolecular ionic interactions between the highly quaternized groups provided a thermodynamic driving force for microphase separation of the QPM segment from PDMS and PHFBMA. And intermolecular van der Waals interactions associated with the long alkyl chains in QAS groups may also contribute to the driving force for microphase separation [9,31]. Surface segregation of low surface tension fluorinated segments may be an additional driving force for microphase separation [30].

Sample PDMS-QPM$_{80}$-PF$_{30}$ exhibited an obvious microphase separation on its surface. Further increase of fluorinated segment contents for sample PDMS-QPM$_{80}$-PF$_{52}$ and PDMS-QPM$_{80}$-PF$_{70}$ showed relatively smooth surface (R_q = 2.12 nm and 1.07 nm, respectively). As discussed in XPS results, the PHFBMA blocks showed weaker migration ability to surface than PDMS and QAS related blocks due to the symmetrical CBABC structure. Therefore, parts of the PHFBMA segments could be entrapped in the copolymer matrix. Subsequently, surface segregation of low surface tension fluorinated segments resulted in reduction of the surface roughness. Moreover, as seen from topography and phase images, the film surfaces of the samples containing fluorinated blocks are much smoother than PDMS-QPM$_{80}$, because of the film-forming ability of PHFBMA blocks [14,28].

The film surface morphologies of the fluorosilicone multi-block copolymers were also viewed under SEM. As shown in the SEM images, the PDMS-QPM$_{80}$ film revealed some pores with uniform sized diameter about 60–80 nm embedded in the copolymer matrix [Fig. 6(a)]. The SEM images also indicated that the pores were transformed into valleys in the PDMS-QPM-PF films (PDMS-QPM$_{80}$-PF$_{30}$ and PDMS-QPM$_{80}$-PF$_{52}$), and disappeared in the film PDMS-QPM$_{80}$-PF$_{70}$ [Fig. 6(b–d)]. Subsequently, wrinkles were generated on the surface of PDMS-QPM$_{80}$-PF$_{70}$ due to the migration of fluorine segments and the film-forming ability of PHFBMA. This phenomenon was coincident with the above discussion about the smallest roughness of PDMS-PM$_{80}$-PF$_{70}$ in AFM. It was assumed that the multi-block copolymers PDMS-QPM-PF containing PHFBMA units were beneficial for the film formation.

3.5. Wettability of the multi-block copolymer films

It is well-known that surface adhesion is strongly dependent on the surface properties, especially wettability [32]. In this study, the surface wettability of the multi-block copolymer was investigated in the measurements of CA, surface energy and CAH. PDMS film was obtained through crosslinking and measured as control. In Fig. 7(a), the surface wettability measurements done on copolymer films showed decreased contact angles in comparison with PDMS, which is mainly due to the quaternary ammonium charged groups in the copolymer films. The QAS alkyl side chains on the film surface tended to fold back and the positively charged nitrogen atoms would be exposed in humid environments, resulting in the increase of hydrophilicity [8]. The CA values of copolymer films were above 90° before immersion in water because of the contribution of the hydrophobic components (PHFBMA and PDMS). The hydroxyl groups in PHEMA units were intended to involve in the crosslink reaction in preparation of the films, and the effect on the CA results could be negligible. The CA values slightly increased with the PHFBMA content in the copolymers due to the hydrophobicity of the fluorine moieties. After immersion in water, the CA values tended to become smaller for all the film surfaces, which were caused by the migration of QAS groups

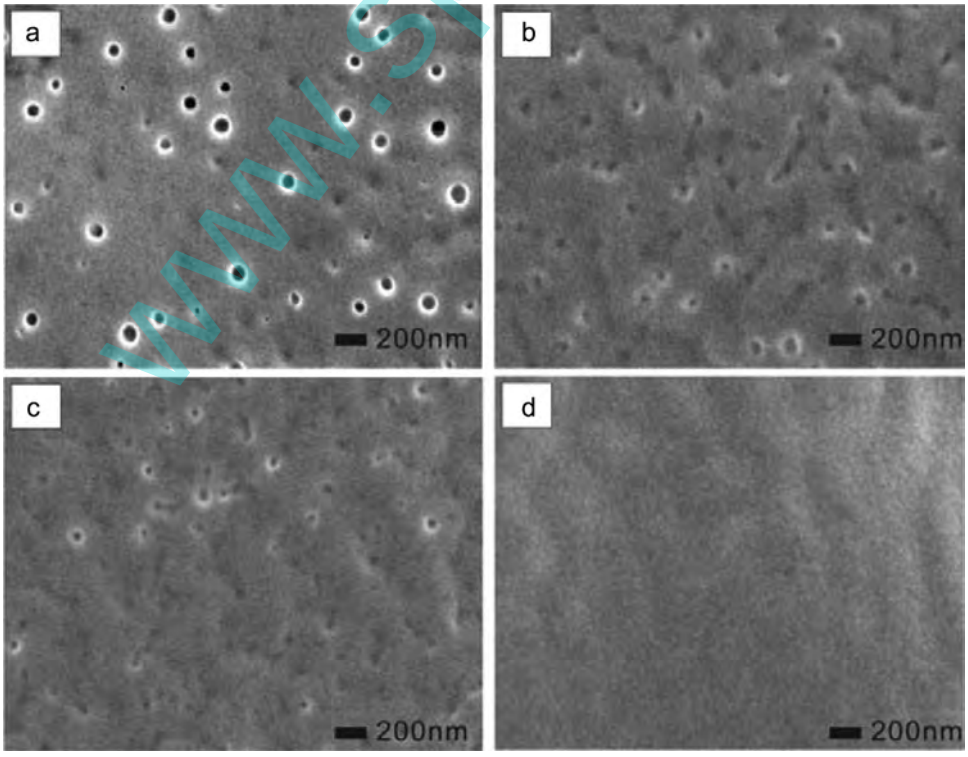

Fig. 6. SEM images of the multi-block copolymer films. (a) PDMS-QPM$_{80}$, (b) PDMS-QPM$_{80}$-PF$_{30}$, (c) PDMS-QPM$_{80}$-PF$_{52}$ and (d) PDMS-QPM$_{80}$-PF$_{70}$.

toward the surface. The CA value of PDMS-QPM$_{80}$ decreased by 9° in magnitude after contacting with water, whereas the CA value of PDMS-QPM$_{80}$-PF$_{52}$ decreased by 15°, due to the difference of the surface QPM segment content. As shown in the XPS test, the surface of PDMS-QPM$_{80}$-PF$_{52}$ possessed the highest C—N$^+$ percentage among others, indicating significant hydrogen bond between cationic groups and water. Therefore, the CA value decreased in the maximum extent after contacting with water. Corresponding to the CA values, surface energy values of the block copolymer films decreased from 24.1 mN/m to 22.5 mN/m, with the increasing order of PHFBMA content [Fig. 7(b)]. After immersion in water, the values of surface energy increased dramatically, which were mainly dominated by reorganization of the fluorosilicone blocks and the QAS groups on the film surface.

The CAH value provided a measurement of the stability for the film surface upon exposure to water [9]. It has been discussed that surface morphology and heterogeneity affect the CAH value [33]. The multi-block copolymer films resulted in variations in surface roughness and/or surface composition after contacting with water and the films exhibited larger CAH than pure PDMS film [Fig. 7(c)]. In addition, with the increased mass percentage of PHFBMA, the values of CAH slightly decreased to 61.5° before contacting with water, corresponding to the variation trend of film surface roughness, i.e. R_q decreased from 4.94 nm to 1.07 nm as PHFBMA content increased. Higher values of CAH also indicated the reorganization of QAS groups on film surfaces due to molecular interactions between QAS groups and water, and this may improve the antimicrobial properties of block copolymer films to some extent [9].

3.6. Antimicrobial activity of the multi-block copolymer films

The antimicrobial activity of the films was evaluated toward the Gram-positive bacteria, *B. subtilis* and Gram-negative bacteria, *E. coli*, respectively, using the agar plating method as described in Fig. 8. Transparent inhibition zones around the coated specimens indicated that PDMS-QPM$_{80}$, PDMS-QPM$_{80}$-PF$_{30}$ and PDMS-QPM$_{80}$-PF$_{52}$ copolymer films had antimicrobial activity toward both *B. subtilis* and *E. coli*, while the effect on PDMS-QPM$_{80}$-PF$_{70}$ film was not distinct.

Surface morphology seemingly exhibits close relationship with the antimicrobial activity, and the prominent role it plays in microorganism adhesion behaviors has been noticed [34–36]. Compared with the surface roughness and topography of the block copolymers, the films of PDMS-QPM$_{80}$ and PDMS-QPM$_{80}$-PF$_{30}$ had the larger roughness values (R_q = 4.94 nm and 4.26 nm, respectively). Consequently the QAS groups on the heterogeneous surface could sufficiently interfere with bacteria by the increased contact area. Relatively, with lower surface roughness value, film PDMS-QPM$_{80}$-PF$_{52}$ (R_q = 2.12 nm) showed more obvious antimicrobial activity. As mentioned previously, with the mass percentage of PHFBMA increased from 0 to 26.1%, surface percentage of C-N$^+$ increased from 67% to 79%, i.e. a certain content of PHFBMA was beneficial for increase the surface percentage of C—N$^+$. It is consistent with the results of Russell et al., who had found that for quaternized PDMAEMA-coated surfaces, the primary factor in the antimicrobial activity is the density of positive charges on the surface rather than polymer chain length or other properties [35,36]. This means more positive charges on the surface improves the ability of the copolymers to interact with the cell wall of the microorganisms and improves antimicrobial activity. Meanwhile, the transparent inhibition zone was not significant in PDMS-QPM$_{80}$-PF$_{70}$ film, which had the lowest surface percentage of C—N$^+$ corresponded to C—N (60%) and the lowest surface roughness values (R_q = 1.07 nm).

Therefore, the antimicrobial activity had close relationship with surface morphology and surface chemical composition. The positive charges on film surface would be the most important for the antimicrobial activity and a certain percentage of PHFBMA was beneficial for increasing surface content of C—N$^+$, and consequently improving antimicrobial activity. The antimicrobial activity depends on the density of positive charges on film surface, which is affected by the particular surface structure of copolymers, and further investigation is under way.

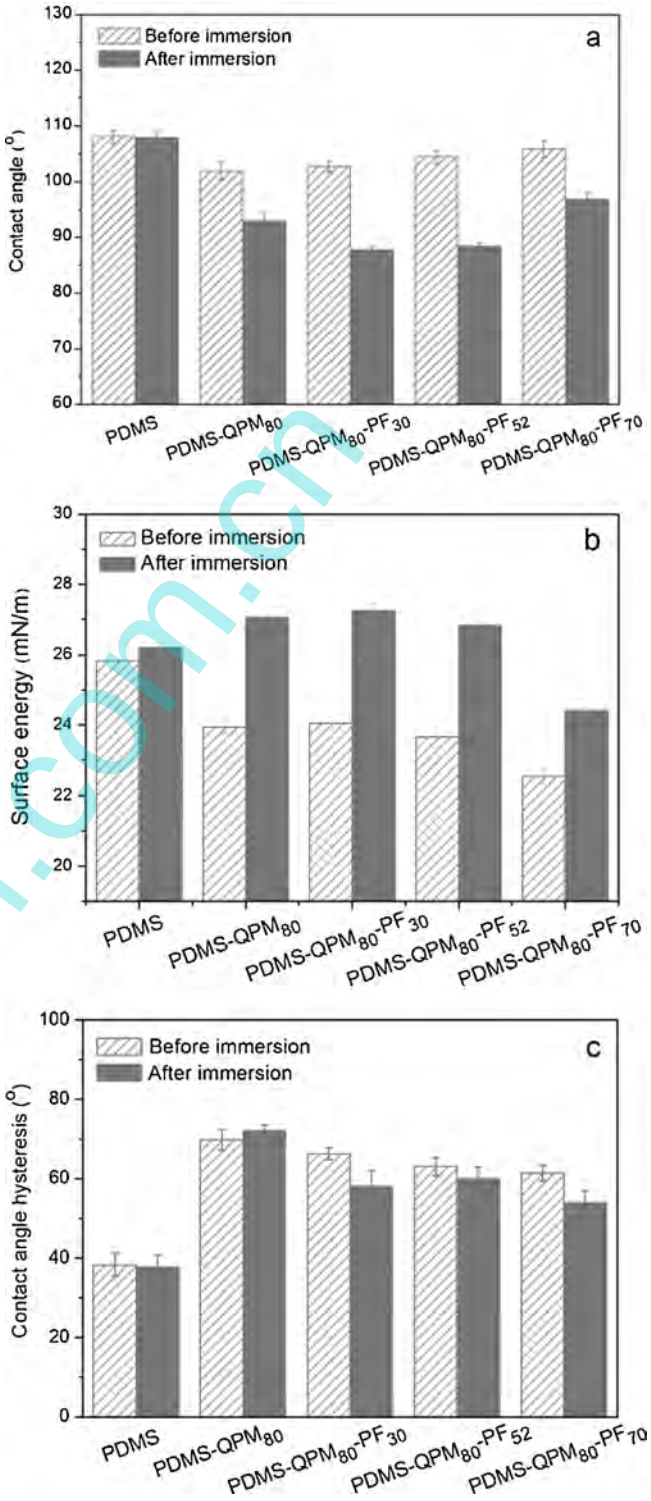

Fig. 7. Water contact angles (a), surface energy (b) and contact angle hysteresis (c) on the multi-block copolymer films before and after immersion in water (mean ± SD, $n \geq 5$).

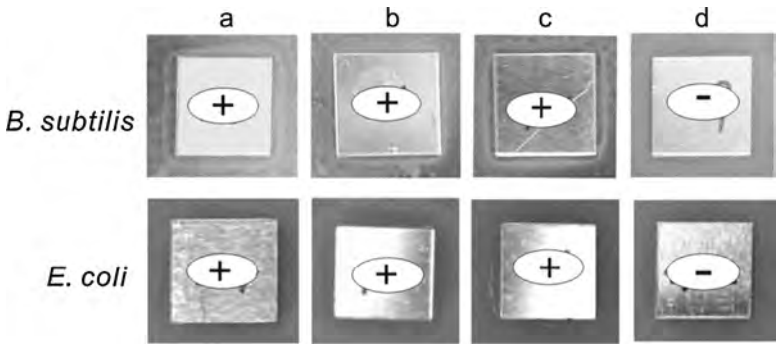

Fig. 8. Antimicrobial activity of the multi-block copolymer films. (a) PDMS-QPM$_{80}$, (b) PDMS-QPM$_{80}$-PF$_{30}$, (c) PDMS-QPM$_{80}$-PF$_{52}$ and (d) PDMS-QPM$_{80}$-PF$_{70}$.

4. Conclusion

A variety of new multi-block copolymers containing QAS groups and fluorosilicone segments were synthesized by RAFT polymerization. The obtained well-defined copolymers with PDMS, PHFBMA and QAS tethered blocks showed special chemical composition and morphology on their film surfaces associated with the symmetrical CBABC chemical structure. The PDMS and QAS related blocks had a stronger tendency migrating to surface than the PHFBMA blocks. With the increase of the mass percentage of PHFBMA, surface roughness values decreased with tendency to form a smooth surface. Surface chemical composition and surface wettability were strongly dependent on the PHFBMA block content. On account of both the surface property and antimicrobial activity, the fluorosilicone multi-block copolymer containing suitable amount of PHFBMA (f_{PHFBMA} < 26.1 wt%) with higher C—N$^+$ content and relatively smooth morphology would find their potential applications in antimicrobial coatings.

Acknowledgment

The authors thank Dr. Jing An in Hebei University of Science and Technology, China, for her help in the antimicrobial test.

References

[1] A. Kugela, S. Stafslien, B.J. Chisholm, Antimicrobial coatings produced by tethering biocides to the coating matrix: a comprehensive review, Prog. Org. Coat. 72 (2011) 222–252.
[2] D.M. Morens, G.K. Folkers, A.S. Fauci, The challenge of emerging and re-emerging infectious diseases, Nature 430 (2004) 242–249.
[3] H. Lu, L. Yu, Q.M. Liu, J.X. Du, Ultrafine silver nanoparticles with excellent antibacterial efficacy prepared by a handover of vesicle templating to micelle stabilization, Polym. Chem. 4 (2013) 3448–3452.
[4] C.H. Gu, H. Zhang, M.D. Lang, Preparation of mono-dispersed silver nanoparticles assisted by chitosan-*g*-poly(ε-caprolactone) micelles and their antimicrobial application, Appl. Surf. Sci. 301 (2015) 273–279.
[5] Z.Q. Cao, L. Mi, J. Mendiola, J.R. Ella-Menye, L. Zhang, H. Xue, S.Y. Jiang, Reversibly switching the function of a surface between attacking and defending against bacteria, Angew. Chem. Int. Ed. 51 (2012) 2602–2605.
[6] C.M. Santos, A. Kumar, S.S. Kolar, R. Contreras-Caceres, A. McDermott, C.Z. Cai, Immobilization of antimicrobial peptide IG-25 onto fluoropolymers *via* fluorous interactions and click chemistry, ACS Appl. Mater. Inter. 5 (2013) 12789–12793.
[7] D.D. Yao, Y.J. Guo, S.G. Chen, J.N. Tang, Y.M. Chen, Shaped core/shell polymer nanoobjects with high antibacterial activities *via* block copolymer microphase separation, Polymer 54 (2013) 3485–3491.
[8] Y.W. Liu, C. Leng, B. Chisholm, S. Stafslien, P. Majumdar, Z. Chen, Surface structures of PDMS incorporated with quaternary ammonium salts designed for antibiofouling and fouling release applications, Langmuir 29 (2013) 2897–2905.
[9] P. Majumdar, E. Lee, N. Gubbins, S.J. Stafslien, J. Daniels, C.J. Thorson, B.J. Chisholm, Synthesis and antimicrobial activity of quaternary ammonium-functionalized POSS (Q-POSS) and polysiloxane films containing Q-POSS, Polymer 50 (2009) 1124–1133.
[10] A.M. Carmona-Ribeiro, L.D. de Melo Carrasco, Cationic antimicrobial polymers and their assemblies, Int. J. Mol. Sci. 14 (2013) 9906–9946.
[11] A.A. Thorpe, V. Peters, J.R. Smith, T.G. Nevell, J. Tsibouklis, Poly (methylpropenoxyfluoroalkylsiloxane)s: a class of fluoropolymers capable of inhibiting bacterial adhesion onto surfaces, J. Fluorine Chem. 104 (2000) 37–45.
[12] T. Cai, W.J. Yang, K.G. Neoh, E.T. Kang, Poly(vinylidene fluoride) membranes with hyperbranched antifouling and antibacterial polymer brushes, Ind. Eng. Chem. Res. 51 (2012) 15962–15973.
[13] D. Park, C.J. Weinman, J.A. Finlay, B.R. Fletcher, M.Y. Paik, H.S. Sundaram, M.D. Dimitriou, K.E. Sohn, M.E. Callow, J.A. Callow, D.L. Handlin, C.L. Willis, D.A. Fischer, E.J. Kramer, C.K. Ober, Amphiphilic surface active triblock copolymers with mixed hydrophobic and hydrophilic side chains for tuned marine fouling-release properties, Langmuir 26 (2010) 9772–9781.
[14] C.M. Guan, Z.H. Luo, J.J. Qiu, P.P. Tang, Novel fluorosilicone triblock copolymers prepared by two-step RAFT polymerization: Synthesis, characterization, and surface properties, Eur. Polym. J. 46 (2010) 1582–1593.
[15] E. Martinelli, M.K. Sarvothaman, M. Alderighi, G. Galli, E. Mielczarski, J.A. Mielczarski, PDMS network blends of amphiphilic acrylic copolymers with poly (ethylene glycol)-fluoroalkyl side chains for fouling-release coatings. I. Chemistry and stability of the film surface, J. Polym. Sci. Polym. Chem. 50 (2012) 2677–2686.
[16] F.J. Xu, H.Z. Li, J. Li, Z.X. Zhang, E. Kang, K. Neoh, Pentablock copolymers of poly(ethylene glycol), poly((2-dimethyl amino) ethyl methacrylate) and poly(2-hydroxyethyl methacrylate) from consecutive atom transfer radical polymerizations for non-viral gene delivery, Biomaterials 29 (2008) 3023–3033.
[17] H.X. Fang, S.X. Zhou, L.M. Wu, Microphase separation behavior on the surfaces of PEG-MDI-PDMS multiblock copolymer coatings, Appl. Surf. Sci. 253 (2006) 2978–2983.
[18] T.C. Ngo, R. Kalinova, D. Cossement, E. Hennebert, R. Mincheva, R. Snyders, P. Flammang, P. Dubois, R. Lazzaroni, P. Leclère, Modification of the adhesive properties of silicone-based coatings by block copolymers, Langmuir 30 (2014) 358–368.
[19] L.C. Paslay, B.A. Abel, T.D. Brown, V. Koul, V. Choudhary, C.L. McCormick, S.E. Morgan, Antimicrobial poly(methacrylamide) derivatives prepared *via* aqueous RAFT polymerization exhibit biocidal effciency dependent upon cation structure, Biomacromolecules 13 (2012) 2472–2482.
[20] Y.F. Zhao, L.P. Zhu, J.H. Jiang, Z. Yi, B.K. Zhu, Y.Y. Xu, Enhancing the antifouling and antimicrobial properties of poly (ether sulfone) membranes by surface quaternization from a reactive poly (ether sulfone) based copolymer additive, Ind. Eng. Chem. Res. 53 (2014) 13952–13962.
[21] X.S. Qin, Y.C. Li, F. Zhou, L.X. Ren, Y.H. Zhao, X.Y. Yuan, Polydimethylsiloxane-polymethacrylate block copolymers tethering quaternary ammonium salt groups for antimicrobial coating, Appl. Surf. Sci. 328 (2015) 183–192.
[22] S.H. Thang, R.T. Mayadunne, G. Moad, E. Rizzardo, A novel synthesis of functional dithioesters, dithiocarbamates, xanthates and trithiocarbonates, Tetrahedron Lett. 40 (1999) 2435–2438.
[23] S. Boileau, L. Bouteiller, A. Kowalewska, Telechelic polydimethylsiloxanes with terminal acetylenic groups prepared by phase-transfer catalysis, Polymer 44 (2003) 6449–6455.
[24] M.L. Wadley, K.A. Cavicchi, Synthesis of polydimethylsiloxane-containing block copolymers *via* reversible addition fragmentation chain transfer (RAFT) polymerization, J. Appl. Polym. Sci. 115 (2010) 635–640.
[25] P. Majumdar, J. He, E. Lee, A. Kallam, N. Gubbins, S.J. Stafslien, J. Daniels, B.J. Chisholm, Antimicrobial activity of polysiloxane coatings containing quaternary ammonium-functionalized polyhedral oligomeric silsesquioxane, J. Coat. Technol. Res. 7 (2010) 455–467.
[26] D. Roy, J.S. Knapp, J.T. Guthrie, S. Perrier, Antibacterial cellulose fiber *via* RAFT surface graft polymerization, Biomacromolecules 9 (2008) 91–99.
[27] W. Zhao, P. Fonsny, P. FitzGerald, G.G. Warr, P. Sebastien, Unexpected behavior of polydimethylsiloxane/poly(2-(dimethylamino)ethyl acrylate) (charged) amphiphilic block copolymers in aqueous solution, Polym. Chem. 4 (2013) 2140–2150.
[28] B. Li, X.H. Li, K.Q. Zhang, H. Li, Y.H. Zhao, L.X. Ren, X.Y. Yuan, Synthesis of POSS-containing fluorosilicone block copolymers *via* RAFT polymerization for application as non-wetting coating materials, Prog. Org. Coat. 78 (2015) 188–199.

[29] S. Karamdoust, B. Yu, C.V. Bonduelle, Y. Liu, G. Davidson, G. Stojcevic, J. Yang, W.M. Lau, E.R. Gillies, Preparation of antibacterial surfaces by hyperthermal hydrogen induced cross-linking of polymer thin films, J. Mater. Chem. 22 (2012) 4881–4889.
[30] W. Yang, L.Q. Zhu, Y.C. Chen, Synthesis and characterization of core-shell latex: Effect of fluorinated acrylic monomer on properties of polyacrylates, J. Fluorine Chem. 157 (2014) 35–40.
[31] Z. Huang, Y. Yu, Y. Huang, Ion aggregation in the polysiloxane ionomers bearing pendant quaternary ammonium groups, J. Appl. Polym. Sci. 83 (2002) 3099–3104.
[32] K. Li, P.P. Wu, Z.W. Han, Preparation and surface properties of fluorine-containing diblock copolymers, Polymer 43 (2002) 4079–4086.
[33] V. Mortazavi, R.M. D'Souza, M. Nosonovsky, Study of contact angle hysteresis using the Cellular Potts Model, Phys. Chem. Chem. Phys. 15 (2013) 2749–2756.
[34] L.C. Hsu, J. Fang, D.A. Borca-Tasciuc, R.W. Worobo, C.I. Moraru, Effect of micro and nanoscale topography on the adhesion of bacterial cells to solid surfaces, Appl. Environ. Microbiol. 79 (2013) 2703–2712.
[35] J.Y. Huang, R.R. Koepsel, H. Murata, W. Wu, S. Lee, T. Kowalewski, A.J. Russell, K. Matyjaszewski, Nonleaching antibacterial glass surfaces *via* grafting onto: the effect of the number of quaternary ammonium groups on biocidal activity, Langmuir 24 (2008) 6785–6795.
[36] H. Murata, R.R. Koepsel, K. Matyjaszewski, A.J. Russell, Permanent, non-leaching antibacterial surfaces-2: how high density cationic surfaces kill bacterial cells, Biomaterials 28 (2007) 4870–4879.